JOURNAL OF AIRCRAFT
Vol. 46, No. 5, September–October 2009

Engineering Notes

Effects of Surface Flats on the Performance of a Remotely Piloted Aircraft

Thomas Nix,* Kenneth Toro,* and Lance W. Traub†
Embry-Riddle Aeronautical University, Prescott, Arizona 86301

DOI: 10.2514/1.44124

Introduction

THE characterization of the aerodynamic performance of airfoils has been the subject of focused study since the 1910s. An implicitly assumed requirement is that the model fidelity (experimental or computational) is such that it is an exact rendering of the proposed full-scale flight article. In many instances, however, the actual wing profile may not be representative of its design. Generally, this becomes a greater issue as the size and dimensions of the vehicle reduce. With the proliferation of small-scale unmanned aerial vehicles, such concerns have increased in relevance. Wing geometry deviations may be due to damage, poor assembly, or simplified structure and design. This is commonly seen in radio-controlled (R/C) aircraft. Weight and cost considerations result in aircraft composed largely of balsa and plywood with a MonoKote skin covering. Generally, the wing skin is not supported between the ribs or the leading- and trailing-edge spars. This naturally results in flats when the skin is attached and stressed. As a result, the airfoil design and that actually implemented on the aircraft may be significantly different. Although wing/airfoil contour issues or alterations due to effects such as battle damage [1,2] have been investigated, little information appears available on a systematic study of contour effects that may result from R/C modeling techniques.

Consequently, a low-speed wind-tunnel investigation has been undertaken to quantify the effect of surface flats on the behavior of a Clark-Y airfoil. Data presented include surface pressure, wake survey, integral lift and drag coefficients, and surface flow visualization.

Equipment and Procedure

A low-speed 1 by 1 ft open-return wind tunnel was used. Wings were designed in CATIA and then rapid-prototyped using Embry-Riddle's rapid-prototyping facilities, yielding acrylonitrile butadiene styrene plastic wing representations. Two 101.6 mm chord c wings were manufactured and pressure-tapped (see Fig. 1). The wing section was a Clark-Y. The profile was chosen due to its wide spread use in the R/C community and good performance at low Reynolds numbers. The so-called modified wing was composed of flats on the upper and lower surfaces, consistent with typical R/C modeling construction technique (see Fig. 1). Note that for larger-scale R/C models, thin sheeting may be used to cover the upper leading edge to approximately 30% chord so that flats in this critical region are avoided. The wings spanned the tunnel to facilitate two-dimensional flow. The tappings were arranged in a diagonal at 20 deg to avoid causing transition. A total of 30 taps were used: 20 on the upper surface and 10 on the lower surface. The tubing used for the ports had an internal diameter of 0.8 mm. Care was taken to ensure that the taps were clean and did not protrude from the surface. The taps were formed by passing Tygon® tubing of the appropriate internal diameter through a preformed location hole in the rapid-prototyped wing surface. The tubing was then bonded in place on the inside of the wing and then cut to length using a thin blade held parallel to the surface. This method resulted in cleanly formed pressure taps that were flush with the surface. Locations of the pressure taps are given in Table 1, in which x/c corresponds to locations along the chord length, and u and l correspond to the upper and lower surfaces, respectively. The wake was surveyed using a 26-port rake wake with a vertical spacing of 2.3 mm. The rake was placed approximately 3 chord lengths downstream of the wing's trailing edge. At this location, the wake static pressure should have relaxed to freestream.

An electronic pressure scanner designed and built in-house was use to acquire pressure data. The scanner consists of 30 independent temperature-compensated differential pressure transducers. A custom interface was written in Visual Basic to process and record the measured pressures. The pressure transducer outputs were digitized using a 32-channel 16-bit National Instruments external universal serial bus analog-to-digital converter board. The board allows scanning of the pressures at up to 250,000 readings/second. All presented pressures are the average of 1000 readings. Calibration of the scanner was performed using a FlowKinetics LLC FKT 1DP1A-SV pressure/flow meter. The FKT meter was calibrated against a deadweight primary standard and was within its calibration specifications. Calibration and comparison of the scanner with the FKT meter showed measured pressure agreement within 0.8 Pa for all 30 of the transducers. The uncertainty interval [3] for the pressure coefficient, lift coefficient, and drag coefficient are 0.011, 0.014, and 0.0022, respectively.

The tunnel freestream velocity was measured using the FlowKinetics LLC FKT 1DP1A-SV meter. This meter measures atmospheric pressure, temperature, and relative humidity, all of which are used to compute the density used in the velocity calculation. The tests were conducted at 36.5 m/s, yielding a Reynolds number of 200,000. Meter accuracy is specified by the manufacturer as better than 0.1%. The wing angle of attack was set using a MD SmartTool digital protractor with a resolution of 0.1 deg. Wing set repeatability was also found to be within 0.1 deg. As the tests are essentially comparative, no corrections for wall effects were applied.

Results and Discussion

In the following discussion, the modified airfoil refers to that with flats. Figures 2 and 3 show a data summary composed of upper surface pressures, wake dynamic pressure defects, and lift and drag coefficient plots (determined through integration of pressures). The effect of the upper surface flats is seen to be one of decambering the airfoil indicated through a positive zero-lift angle-of-attack shift of approximately 1 deg and a marginal change of the lift-curve slope (see Fig. 2a). The stall, however, appears to be favorably affected by the flats.

At an angle of attack of −4 deg (Fig. 2b), the upper surface pressure distribution is similar for both wings. At this incidence, the upper surface is the pressure side; consequently, the flats have a reduced impact on the flow. However, the lower surface pressure coefficients are more negative on the modified airfoil, which tends to

Received 3 March 2009; revision received 10 April 2009; accepted for publication 11 April 2009.

*Undergraduate Student, Aerospace and Mechanical Engineering Department.
†Associate Professor, Aerospace and Mechanical Engineering Department. Member AIAA.

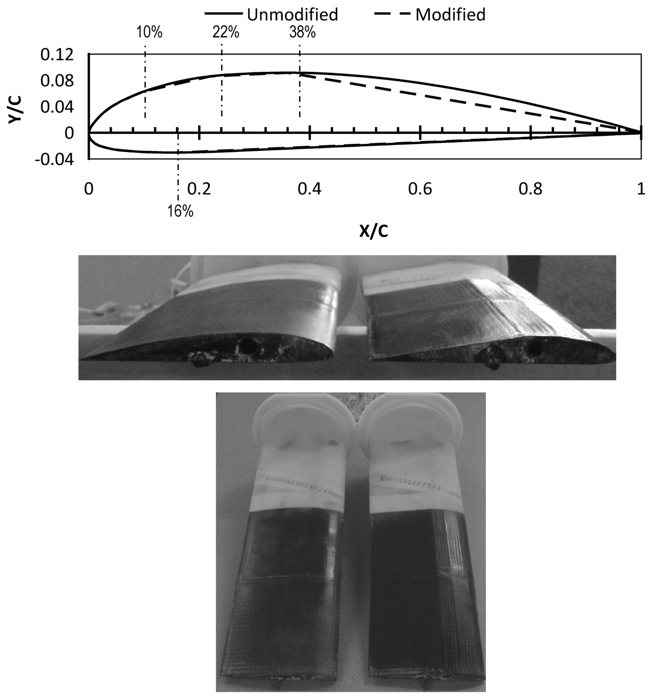

Fig. 1 Clark *Y* model geometric details. Percentages on upper inset indicate locations of flats.

reduce the lift. The lower surface flat appears to causes a drop of pressure just aft of its forward junction. At a 4 deg angle of attack, the upper surface pressure distribution shows a localized separation (bubble) over the extent of the second flat (22–38%). The pressure coefficient drops (more negative) at the bubble onset, due to the external flow accelerating over the separation surface. Attachment appears to occur just aft of the second flat (about 40%). Flow expansion and deceleration to the surface results in increased surface pressure, reducing suction over the aft section, compared with the unmodified wing. The lower surface shows little effect of the flats.

At a 12 deg angle of attack (Fig. 2c), the effect of the upper and lower surface flats on the surface pressure distribution has greatly diminished, as shown in comparison with the unmodified wing. The flats do, however, result in undulations in the plots caused by local separations. At 20 deg incidence, the modified airfoil shows attached flow until about 15% of the chord, followed by massive separation. This results in enhanced performance compared with the unmodified airfoil, which shows massive separation from the first upper surface pressure port aft.

Figure 3 identifies the impact of the flats on the wake momentum deficit as well as the integrated drag coefficient. The drag coefficient C_d was calculated using

$$C_d = \frac{2}{c} \int_{y_{\rm lower}}^{y_{\rm upper}} \sqrt{\frac{q}{qo}} - \frac{q}{qo}\,{\rm d}y \tag{1}$$

where $y_{\rm lower}$ and $y_{\rm upper}$ are the vertical extents of the survey, q is the dynamic pressure, and qo is the freestream dynamic pressure taken as that at the edge of the wake. As may be seen in Fig. 3a, the flats result in a significant increase in the drag coefficient, caused by the areas of localized flow separation. Because of the sparseness of the tapping density in the wake (Fig. 3b), the data in Fig. 3a preclude any strict quantitative assessment. As may be seen in Fig. 3b, the primary effect of the flats is to increase the peak momentum deficit in the wake, while increasing the wake width moderately. Note that the vertical scale in Fig. 3b is not indicative of the wake positioning; the curves were simply arrayed vertically to clarify inspection.

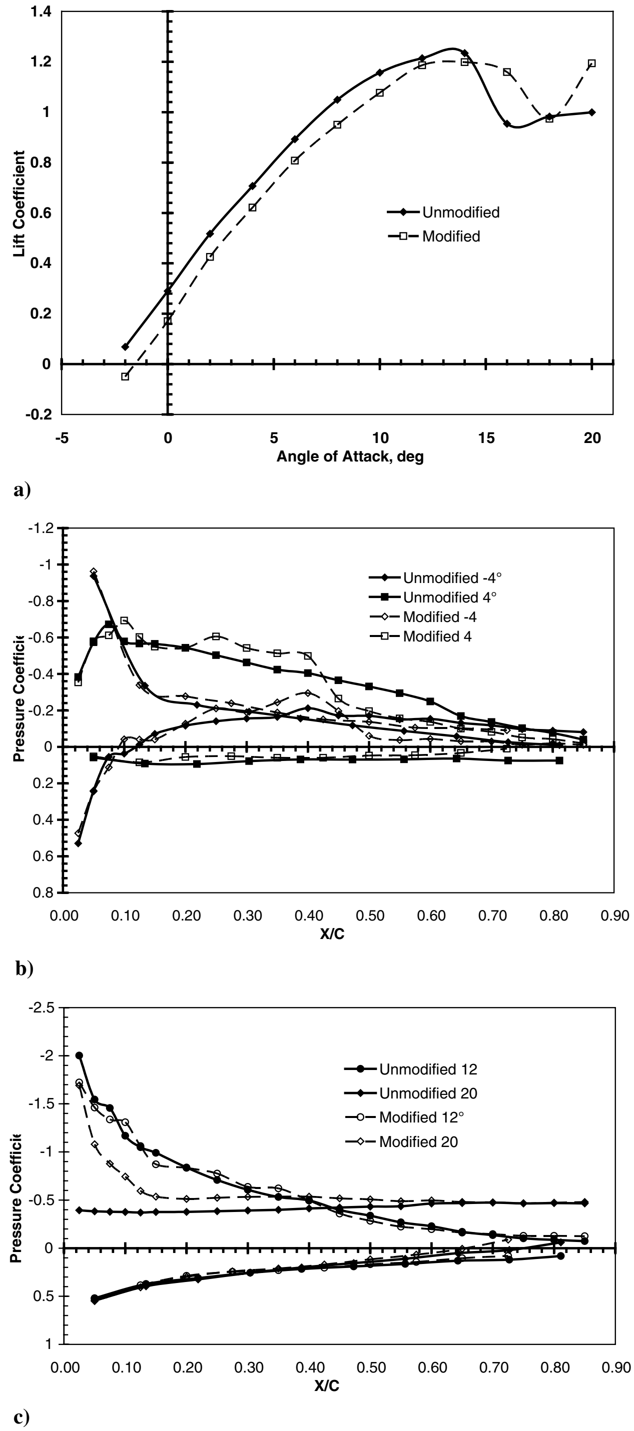

Fig. 2 Effect of surface flats on measured a) lift and pressure coefficient b) and c).

To gain a greater understanding of the flow physics, surface flow visualization was undertaken using surface paint (titanium dioxide, paraffin, and linseed oil). Figure 4 shows the surface skin-friction patterns over the two wings for angles of attack of 0, 6, and 12 deg. At 0 deg incidence, the unmodified wing shows a laminar transitional bubble at approximately 55–75%. The modified airfoil shows a line

Table 1 Pressure port locations

x/c, u	0.03	0.05	0.08	0.1	0.13	0.15	0.2	0.25	0.3	0.35	0.4	0.45	0.5	0.55	0.60	0.65	0.7	0.75	0.8	0.85
x/c, l	0.05	0.13	0.22	0.3	0.39	0.47	0.56	0.64	0.73	0.81										

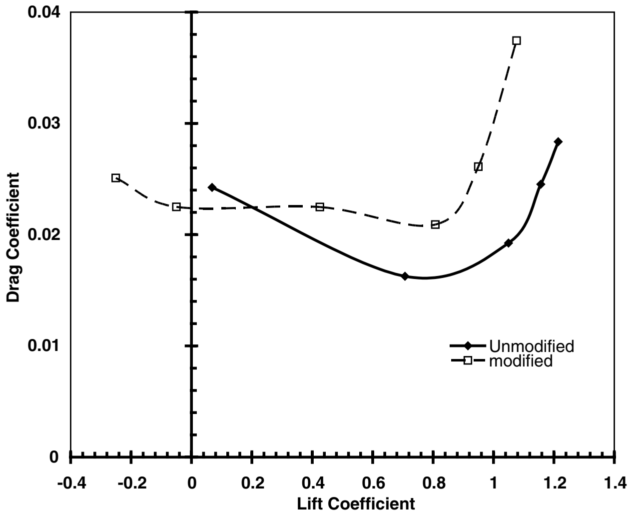

a)

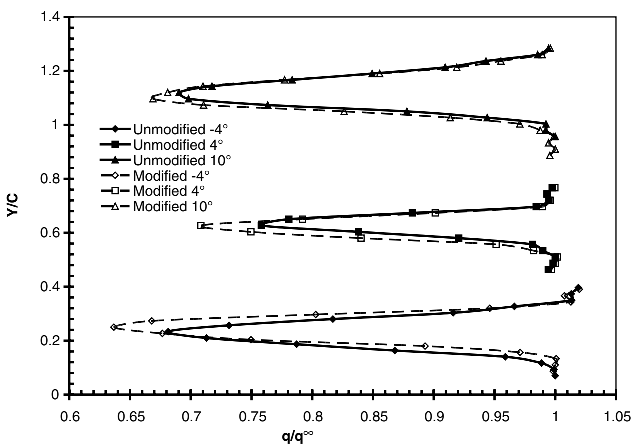

b)

Fig. 3 Effect of surface flats on a) drag coefficient and b) wake profile.

of separation originating from the termination of the second upper surface flat at approximately 38% chord. The separation surface reattaches at approximately 52% chord. What may also be suggested by the apparent scrubbing at the end of the first flat (22% chord) is that this discontinuity appears to promote boundary-layer transition. At 6 deg incidence, the transitional bubble on the unmodified airfoil has moved forward (due to increased adverse pressure recovery demands) and contracted (noted in association with the onset of trailing-edge separation, which is indicated [4]), a well-documented behavior [4,5]. The modified airfoil shows multiple closed separations propagating from the surface discontinuity at the start of each flat. No trailing-edge separation is evident. At 12 deg incidence, both wings show large-scale separated flow. However, the flats on the modified airfoil appear to form a demarcation line dividing the attached flow from the massively separated for this incidence. The uniform line of separation also appears to cause well-defined symmetry with two defined foci of separation divided by a half-saddle.

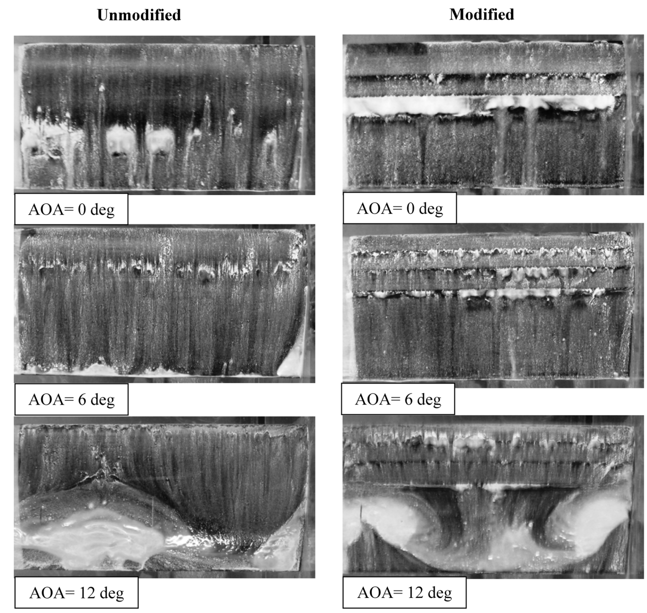

Fig. 4 Surface skin-friction patterns showing the effect of the surface flats compared with the unmodified airfoil (AOA denotes angle of attack).

Conclusions

A low-speed wind-tunnel investigation was undertaken to establish the effect of surface flats, analogous to those resulting from common radio-controlled aircraft modeling techniques. Tests were undertaken at a Reynolds number of 200,000 using two fabricated wings with a Clark-Y profile: one with surface flats and the other representative of the section. The results indicate that the implemented surface flats effectively decamber the airfoil, and so reduce lift, but are beneficial around stall. Obvious effects of the flats on the pressure distribution are seen to diminish, compared with the unmodified wing, as the incidence increases. Drag data indicated a significant drag rise due to the localized separations over the airfoil with flats. Wake traces showed the drag embodiment as a greater peak momentum deficit with a slight increase in the wake width.

References

[1] Render, P. M., Silva, S., Walton, A. J., and Mahmoud, M., "Experimental Investigation into the Aerodynamics of Battle Damaged Airfoils," *Journal of Aircraft*, Vol. 44, No. 2, 2007, pp. 539–549. doi:10.2514/1.24144

[2] Hayes, C., "Effects of Simulated Wing Damage on the Aerodynamic Characteristics of a Swept-Wing Aeroplane Model," NASA TMX-1550, 1968.

[3] Kline, S. J., and McClintock, F. A., "Describing Uncertainties in Single Sample Experiments," *Mechanical Engineering*, Vol. 75, Jan. 1953, pp. 3–8.

[4] Hsiao, F. B., and Hsu, C. C., "Numerical Prediction of Aerodynamic Performance for Low Reynolds Number Airfoils," *Journal of Aircraft*, Vol. 26, No. 7, 1989, pp. 689–691. doi:10.2514/3.45823

[5] Traub, L. W., and Cooper, E., "An Experimental Investigation of Pressure Measurement and Airfoil Characteristics at Low Reynolds Numbers," *Journal of Aircraft*, Vol. 45, No. 4, 2008, pp. 1322–1333. doi:10.2514/1.34769